Author's manuscript, prepublication. Final appeared in Optics Communications **257**, 146-163 (2006).

Quantum mechanics of phase-sensitive amplification in a fiber

C. J. McKinstrie,[1] M. G. Raymer[2], S. Radic[3] and M. V. Vasilyev[4]

[1] *Bell Laboratories, Lucent Technologies, Holmdel, NJ 07733*

[2] *Oregon Center for Optics and Department of Physics, University of Oregon, Eugene, OR 97403*

[3] *Department of Electrical and Computer Engineering, University of California at San Diego, La Jolla, CA 92093*

[4] *Department of Electrical Engineering, University of Texas, Arlington, TX 76010*

Abstract

In a recent paper [Opt. Express **12**, 4973–4979 (2004)] four schemes were described, which produce phase-sensitive amplification in fibers: Degenerate scalar and vector four-wave mixing (FWM), and phase conjugation (PC) combined with frequency conversion (FC), in either order. In this paper the basic quantum mechanics of these schemes are discussed. For each scheme, formulas are derived for the field-quadrature and photon-number variances, which facilitate the (signal and idler) noise-figure analyses for direct and homodyne detection. The effects of polarization misalignment on vector FWM, and the effects of unbalanced conversion on PC combined with FC, are studied. Moderate amounts of these imperfections do not degrade significantly the performances of the aforementioned schemes.

1. Introduction

Long-haul communication systems require optical amplifiers to compensate for fiber loss. Current systems use erbium-doped and Raman fiber amplifiers. These amplifiers are examples of phase-insensitive amplifiers (PIAs), which produce signal gain that is independent of the signal phase. In principle, one could also use phase-sensitive amplifiers (PSAs) in communication systems. The potential advantages of PSAs include, but are not limited to, noise reduction [1], the reduction of noise-induced frequency [2] and phase [3] fluctuations, dispersion compensation [4], and the suppression of the modulational instability [5].

Four-wave mixing (FWM) processes driven by two pump waves, with parallel and perpendicular polarization vectors, in fibers with constant and random birefringence, were reviewed in detail [6, 7, 8, 9]. In a recent paper [10] schemes based on FWM were described, which produce phase-sensitive amplification (also abbreviated as PSA) in fibers: Degenerate scalar and vector FWM, and phase conjugation (PC) combined with Bragg scattering (BS), or frequency conversion (FC), in either order. In this paper the basic quantum mechanics of these schemes are discussed.

This paper is organized as follows: Degenerate scalar FWM is studied in Section 2. If the input signal is a one-mode coherent state, the output signal is a one-mode squeezed coherent state. The characteristics of a such a state are illustrated, and contrasted to the characteristics of the state produced by PIA. Degenerate vector FWM is studied in Section 3. If the polarization vector of the input signal is aligned perfectly, the output signal is a one-mode squeezed state. Cascaded nondegenerate-FWM processes are studied in Section 4. FC followed by PC produces one two-mode squeezed state. In contrast, if the conversion process is balanced, PC followed by FC produces two one-mode squeezed states. The effects of polarization misalignment on degenerate vector FWM are studied in Section 5, and the effects of unbalanced conversion on PC followed by FC are studied in Section 6. Finally, in Section 7 the main results of this paper are summarized.

2. Degenerate scalar four-wave mixing

Degenerate scalar FWM involves two strong pump waves (3 and 1) and a weak signal wave

(2), whose frequencies satisfy the matching condition $\omega_3 + \omega_1 = 2\omega_2$. The frequencies and polarizations of the interacting waves are illustrated in Figure 1. In classical mechanics, the

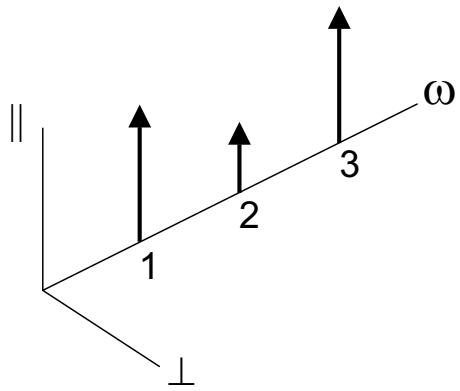

Figure 1: Polarization diagram for degenerate scalar FWM.

initial evolution of degenerate scalar FWM is modelled by the linearized amplitude equation

$$d_z A = i\delta A + i\gamma A^*, \tag{1}$$

where A is the amplitude of wave 2, δ is a real constant that quantifies the wavenumber mismatch and γ is a complex constant that quantifies the nonlinear coupling made possible by the pumps. Formulas for these quantities are stated in [6, 9, 10]. Equation (1) is equivalent to the Hamiltonian

$$H = \delta A^* A + [\gamma (A^*)^2 + \gamma^* A^2]/2, \tag{2}$$

together with the Hamilton equation-of-motion

$$d_z A = i\partial H/\partial A^*. \tag{3}$$

The solution of Eq. (1) can be written in the input-output form

$$A(z) = \mu(z)A(0) + \nu(z)A^*(0), \tag{4}$$

where the transfer functions

$$\mu(z) = \cosh(\kappa z) + i(\delta/\kappa)\sinh(\kappa z), \tag{5}$$

$$\nu(z) = i(\gamma/\kappa)\sinh(\kappa z) \tag{6}$$

and the growth rate $\kappa = (|\gamma|^2 - \delta^2)^{1/2}$. For reference, the transfer functions satisfy the auxiliary equation $|\mu|^2 - |\nu|^2 = 1$.

In quantum mechanics [11], degenerate scalar FWM is modelled by the Hamiltonian

$$H_s = \delta a_s^\dagger a_s + [\gamma (a_s^\dagger)^2 + \gamma^* a_s^2]/2, \tag{7}$$

together with the Schrödinger equation-of-motion

$$-i d_z |\psi_s\rangle = H_s |\psi_s\rangle, \tag{8}$$

where a_s is the Schrödinger operator associated with mode 2, δ and γ are the aforementioned constants, and $|\psi\rangle$ is the wave function (state vector). In the Schrödinger picture the state vector evolves according to the equation

$$|\psi_s(z)\rangle = U(z)|\psi(0)\rangle, \tag{9}$$

where the evolution (transformation) operator $U(z) = e^{iH_s z}$, and the mode operator a_s is constant. In the Heisenberg picture the state vector $|\psi_h\rangle$ is constant and the mode operator a_h evolves according to the equation

$$a_h(z) = U^\dagger(z) a(0) U(z). \tag{10}$$

Equations (7) and (8) are equivalent to the Hamiltonian

$$H_h = \delta a_h^\dagger a_h + [\gamma (a_h^\dagger)^2 + \gamma^* a_h^2]/2, \tag{11}$$

together with the Heisenberg equation-of-motion

$$d_z a_h = i[a_h, H_h]. \tag{12}$$

By combining Eqs. (11) and (12), one finds that

$$d_z a_h = i\delta a_h + i\gamma a_h^\dagger. \tag{13}$$

Henceforth, the subscripts h and s will be suppressed. The picture should be clear from the context.

Because the Heisenberg mode operator obeys the same differential equation as the classical wave amplitude, the transfer functions (5) and (6) also characterize the quantum mechanics of degenerate scalar FWM. The input-output relation

$$a(z) = \mu(z)a(0) + \nu(z)a^\dagger(0) \tag{14}$$

is a one-mode squeezing transformation [12, 13], which is parameterized by δz (real) and γz (complex). The auxiliary equation $|\mu|^2 - |\nu|^2 = 1$ ensures that it is unitary. Because this transformation differs slightly from the textbook transformation ($\delta z \neq 0$ and γz appears instead of $i\zeta$), its basic properties are summarized in Appendix A. Let $\mu = |\mu|e^{i\phi_\mu}$, $\nu = |\nu|e^{i(\phi_\mu+\phi_\nu)}$ and $s = \tanh^{-1}|\nu/\mu|$. Then Eq. (14) can be rewritten in the form

$$a(z) = e^{i\phi_\mu}[\cosh(s)a(0) + \sinh(s)e^{i\phi_\nu}a^\dagger(0)]. \tag{15}$$

Transformation (15) incorporates a phase shift ϕ_μ, stretching by the factor e^s along an axis that is inclined by $\phi_\nu/2$ relative to the real (mode-amplitude) axis and squeezing by the same factor (stretching by the inverse factor e^{-s}) along the perpendicular axis. For reference, ϕ_ν depends on the pump phases, which can be controlled.

Current communication systems are based on coherent signals. The coherent state $|\beta\rangle = D(\beta)|0\rangle$, where β is the coherent displacement, $D(\beta)$ is the coherent-displacement operator and $|0\rangle$ is the vacuum state. If such a state is the input to a four-wave mixer, the output is the squeezed coherent state $S(\gamma,\delta)D(\beta)|0\rangle$, where $S(\gamma,\delta)$ is the squeezing operator associated with Eqs. (7) and (9). The properties of the displacement and squeezing operators are described briefly in Appendix A. It is customary to use the vacuum state as a virtual input state, and to incorporate the displacement required to produce the actual input state in the input-output relation associated with the FWM process. By doing so, one obtains the modified input-output relation

$$a(z) = \alpha + \mu(z)a(0) + \nu(z)a^\dagger(0), \tag{16}$$

where $\alpha = \mu\beta + \nu\beta^*$. Because $a|0\rangle = 0$ and $a^\dagger|0\rangle = |1\rangle$ at the input position 0, it is a simple matter to calculate the operator moments at the output position z. The results are

$$\langle a\rangle \;=\; \alpha, \tag{17}$$

$$\langle a^2\rangle = \alpha^2 + \mu\nu, \tag{18}$$

$$\langle a^\dagger a\rangle = |\alpha|^2 + |\nu|^2, \tag{19}$$

$$\langle (a^\dagger a)^2\rangle = (|\alpha|^2 + |\nu|^2)^2 + |\alpha|^2(|\mu|^2 + |\nu|^2) + \alpha^2(\mu\nu)^* + (\alpha^*)^2\mu\nu + 2|\mu|^2|\nu|^2. \tag{20}$$

Equation (17) identifies α as the output amplitude and a similar equation allows the displacement β to be called the input amplitude. The expected values of the quadrature operators $x = (a + a^\dagger)/2$ and $y = (a - a^\dagger)/2i$, and the number operator $n = a^\dagger a$, follow from Eqs. (17) and (19). By combining Eq. (18) and its conjugate with Eq. (19), one finds that the quadrature variances

$$\langle \delta x^2\rangle = [1 + 2|\nu|^2 + \mu\nu + (\mu\nu)^*]/4, \tag{21}$$

$$\langle \delta y^2\rangle = [1 + 2|\nu|^2 - \mu\nu - (\mu\nu)^*]/4. \tag{22}$$

The number variance follows from Eqs. (19) and (20).

By rewriting the aforementioned variances in terms of the phase and squeezing parameters ϕ_μ, ϕ_ν and s [Eq. (15)], one finds that

$$\langle \delta x^2\rangle = [\exp(2s)\cos^2(\phi_\mu + \phi_\nu/2) + \exp(-2s)\sin^2(\phi_\mu + \phi_\nu/2)]/4, \tag{23}$$

$$\langle \delta y^2\rangle = [\exp(2s)\sin^2(\phi_\mu + \phi_\nu/2) + \exp(-2s)\cos^2(\phi_\mu + \phi_\nu/2)]/4, \tag{24}$$

$$\langle \delta n^2\rangle = |\alpha|^2[\exp(2s)\cos^2(\phi_\mu + \phi_\nu/2 - \phi_\alpha) + \exp(-2s)\sin^2(\phi_\mu + \phi_\nu/2 - \phi_\alpha)] + 2\sinh^2(s)\cosh^2(s), \tag{25}$$

where $\phi_\alpha = \arg(\alpha)$. When $\phi_\mu = 0$, results (23)–(25) reduce to the textbook results [12, 13]. In fiber optics it is customary to define the gain $G = |\mu|^2$, in which case $|\nu|^2 = G - 1$. By using this notation, one can write the output strength- and phase-equations in the form

$$|\alpha|^2 = |\beta|^2\{2G - 1 + 2[G(G-1)]^{1/2}\cos\xi\}, \tag{26}$$

$$\phi_\alpha = \phi_\beta + \phi_\mu + \tan^{-1}\Big[\frac{(G-1)^{1/2}\sin\xi}{G^{1/2} + (G-1)^{1/2}\cos\xi}\Big], \tag{27}$$

where the relative phase $\xi = \phi_\nu - 2\phi_\beta$. The output number

$$\langle n\rangle = |\alpha|^2 + G - 1. \tag{28}$$

One can rewrite the quadrature- and number-variance equations (23)–(25) in the form

$$\langle \delta q^2 \rangle = \{2G - 1 \pm 2[G(G-1)]^{1/2} \cos\eta\}/4, \tag{29}$$

$$\langle \delta n^2 \rangle = |\alpha|^2\{2G - 1 + 2[G(G-1)]^{1/2} \cos\zeta\} + 2G(G-1), \tag{30}$$

where the + sign in Eq. (29) pertains to the x variance, the − sign pertains to the y variance, and the phases $\eta = \phi_\nu + 2\phi_\mu$ and $\zeta = \phi_\nu - 2(\phi_\alpha - \phi_\mu)$. It follows from Eq. (27) and the preceding definition that

$$\zeta = \xi - 2\tan^{-1}\Big[\frac{(G-1)^{1/2}\sin\xi}{G^{1/2} + (G-1)^{1/2}\cos\xi}\Big]. \tag{31}$$

The output strength, phase and number-variance all depend on the relative phase $\phi_\nu - 2\phi_\beta$. In contrast, the output quadrature-variances depend on the coupling phase $\phi_\nu + 2\phi_\mu$, but not the input phase ϕ_β. If the input phase varies, so also does the output amplitude, which is the center of the quantal probability cloud. However, the size, shape and orientation of the probability cloud remain constant [12, 13].

To characteristics of PIA were reviewed in [14]. For reference, the output operator-moments associated with PIA are

$$\langle a \rangle = \alpha, \tag{32}$$

$$\langle a^2 \rangle = \alpha^2, \tag{33}$$

$$\langle a^\dagger a \rangle = |\alpha|^2 + |\nu|^2, \tag{34}$$

$$\langle (a^\dagger a)^2 \rangle = (|\alpha|^2 + |\nu|^2)^2 + |\alpha|^2(|\mu|^2 + |\nu|^2) + |\mu|^2|\nu|^2, \tag{35}$$

where the output amplitude $\alpha = \mu\beta$. The output variances associated with PIA are

$$\langle \delta q^2 \rangle = (1 + 2|\nu|^2)/4, \tag{36}$$

$$\langle \delta n^2 \rangle = |\alpha|^2(|\mu|^2 + |\nu|^2) + |\mu|^2|\nu|^2, \tag{37}$$

where $\langle \delta q^2 \rangle$ represents both the x and y variances. As the term PIA implies, formulas (34)–(37) do not depend on the phase of the input amplitude, or the phases of the transfer coefficients. By using the notation described above, one can write the output strength- and phase-equations in the form

$$|\alpha|^2 = |\beta|^2 G, \tag{38}$$

$$\phi_\alpha = \phi_\beta + \phi_\mu. \tag{39}$$

As implied by Eq. (34), the output number

$$\langle n \rangle = |\alpha|^2 + G - 1. \tag{40}$$

One can rewrite the quadrature- and number-variance equations in the form

$$\langle \delta q^2 \rangle = (2G - 1)/4, \tag{41}$$

$$\langle \delta n^2 \rangle = |\alpha|^2(2G - 1) + G(G - 1). \tag{42}$$

To illustrate the preceding results, it is sufficient to consider the ideal case in which the wavenumber mismatch $\delta = 0$ and, hence, the transfer coefficient μ is real [10]. The following figures all pertain to the case in which the input number $|\beta|^2 = 100$ and the gain $G = 10$. In Figure 2 the output strengths $|\alpha|^2$ and phase shifts $\phi_\alpha - \phi_\beta$ are plotted as functions of the relative phase $\phi_\nu - 2\phi_\beta$. Both output strengths are normalized to the output strength for PIA, which is given by Eq. (38), and both phases are measured in radians. In Figure 3

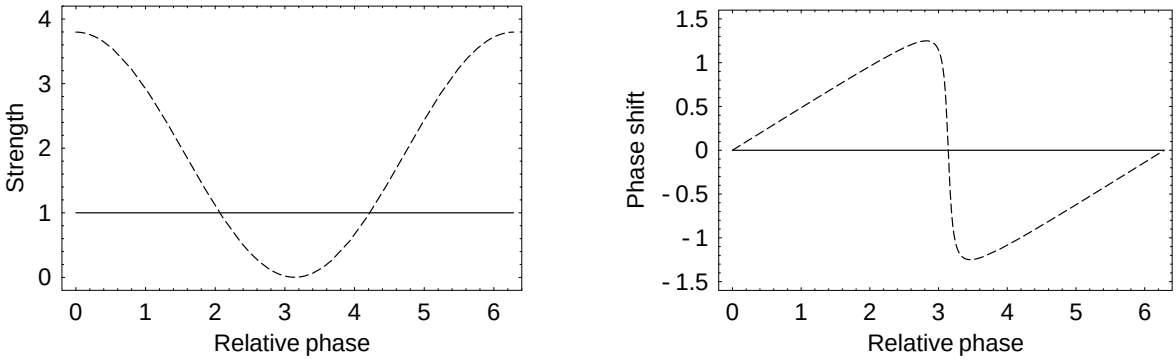

Figure 2: Signal strength and phase shift plotted as functions of the relative phase. The solid lines represent phase-insensitive amplification, whereas the dashed curves represent phase-sensitive amplification.

the quadrature variances are plotted as functions of the coupling phase ϕ_ν and the number variance is plotted as a function of $\phi_\nu - 2\phi_\beta$. All variances are normalized to the variances for PIA, which are given by Eqs. (41) and (42), and both phases are measured in radians. Figure 3*b* might lead one to conclude that out-of-phase amplification produces the least-noisy output. This conclusion is true on an absolute scale, but not on a relative scale. It is useful to define the relative noise (of the signal) as $\langle \delta n^2 \rangle / \langle n \rangle^2$ and the figure of demerit (of the

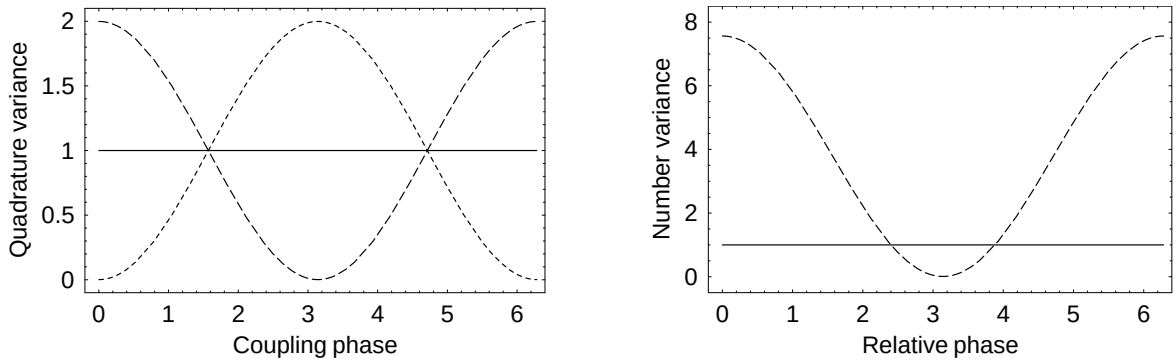

Figure 3: Signal quadrature and number variances plotted as functions of the coupling phase and relative phase, respectively. The solid lines represent phase-insensitive amplification, whereas the dashed and dotted curves represent phase-sensitive amplification. In (a) the dashed curve represents the x variance, whereas the dotted curve represents the y variance.

amplification process) as the output relative noise divided by the input relative noise. These definitions imply that lower figures of demerit are better. For a coherent input, the relative noise is $1/|\beta|^2$. In Figure 4 the figures of demerit associated with PIA and PSA are plotted as functions of $\phi_\nu - 2\phi_\beta$, which is measured in radians. The PIA figure-of-demerit is 2.8 dB,

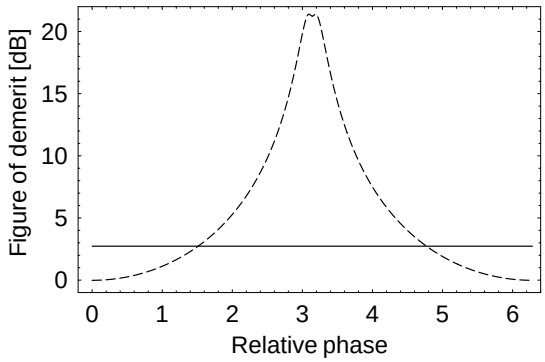

Figure 4: Figures of demerit for phase-insensitive amplification (solid line) and phase-sensitive amplification (dashed curve) plotted as functions of the relative phase.

which is close to the high-gain limit of 3 dB. The PSA figure-of-demerit varies from 0 to 22 dB. It is lowest when the number variance is highest and *vice versa*. Although in-phase amplification produces the highest number variance, it also produces the highest number, so the figure of demerit is a minimum. In contrast, although out-of-phase amplification produces the lowest number variance, it also produces the lowest number, so the figure of

demerit is a maximum.

The preceding definitions of relative noise and figure of demerit coincide with the definitions of noise-to-signal ratio and noise figure associated with direct detection. We used different terminology deliberately, to prevent the misconceptions that direct detection is the only, or best, way to measure squeezed signals. To take full advantage of the characteristics of squeezed signals, one must use balanced homodyne detection [12, 13].

3. Degenerate vector four-wave mixing

Nondegenerate FWM involves two strong pump waves (4 and 1), and weak signal (2) and idler (3) waves, whose frequencies satisfy the matching condition $\omega_4 + \omega_1 = \omega_2 + \omega_3$. In degenerate vector FWM, waves 2 and 3 are the polarization components of a weak signal ($\omega_2 = \omega_3$). The frequencies and polarizations of the interacting waves are illustrated in Figure 5.

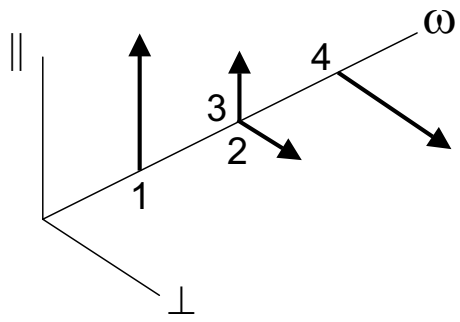

Figure 5: Polarization diagram for degenerate vector FWM.

Let a denote the mode operator of the signal and b denote the operator of the vacuum mode whose polarization vector is orthogonal (perpendicular) to that of the signal. The analysis of FWM driven by perpendicular pumps is facilitated by the introduction of modes 2 and 3, which are polarized parallel to pump 1 and pump 4, respectively. The mode inputs are related by the change-of-basis equations

$$a_2(0) = \bar{\mu} a(0) + \bar{\nu} b(0), \tag{43}$$

$$a_3(0) = -\bar{\nu}^* a(0) + \bar{\mu}^* b(0). \tag{44}$$

The conjugate and minus signs in Eqs. (43) and (44) ensure that mode 3 is perpendicular to mode 2, and the auxiliary equation $|\bar{\mu}|^2 + |\bar{\nu}|^2 = 1$ ensures that the change-of-basis transformation is unitary and conserves photons. Equations (43) and (44) are identical to the beam-splitter equations [12, 13].

Degenerate vector FWM is governed by the Hamiltonian

$$H = i\delta(a_2^\dagger a_2 + a_3^\dagger a_3) + i(\gamma a_2^\dagger a_3^\dagger + \gamma^* a_2 a_3), \tag{45}$$

where γ depends on the pump amplitudes, together with the Heisenberg equations-of-motion

$$d_z a_j = i[a_j, H], \tag{46}$$

where $j = 1$ or 2. Formulas for δ and γ are stated in [7, 8, 9, 10]. By combining Eqs. (45) and (46), one obtains the operator equations

$$d_z a_2 = i\delta a_2 + i\gamma a_3^\dagger, \tag{47}$$

$$d_z a_3^\dagger = -i\gamma^* a_2 - i\delta a_3^\dagger. \tag{48}$$

The solutions of Eqs. (47) and (48) are

$$a_2(z) = \mu(z) a_2(0) + \nu(z) a_3^\dagger(0), \tag{49}$$

$$a_3^\dagger(z) = \nu^*(z) a_2(0) + \mu^*(z) a_3^\dagger(0), \tag{50}$$

where the transfer functions μ and ν were defined in Eqs. (5) and (6), respectively, and satisfy the auxiliary equation $|\mu|^2 - |\nu|^2 = 1$. The input-output relations (49) and (50) describe a two-mode squeezing transformation [12].

The mode outputs are related by the equations

$$a(z) = \bar{\mu}^* a_2(z) - \bar{\nu} a_3(z), \tag{51}$$

$$b(z) = \bar{\nu}^* a_2(z) + \bar{\mu} a_3(z), \tag{52}$$

which are the inverses of Eqs. (43) and (44). By combining the input-output relations with both change-of-basis relations, one finds that

$$a(z) = \mu(|\bar{\mu}|^2 + |\bar{\nu}|^2) a(0) - \nu(2\bar{\mu}^*\bar{\nu}) a^\dagger(0) + \nu(|\bar{\mu}|^2 - |\bar{\nu}|^2) b^\dagger(0), \tag{53}$$

$$b(z) = \nu(|\bar{\mu}|^2 - |\bar{\nu}|^2) a^\dagger(0) + \mu(|\bar{\mu}|^2 + |\bar{\nu}|^2) b(0) + \nu(2\bar{\mu}\bar{\nu}^*) b^\dagger(0). \tag{54}$$

If the parallel and perpendicular components of the input mode have equal magnitudes ($|\bar{\mu}| = |\bar{\nu}| = 1/2$), Eqs. (53) and (54) reduce to

$$a(z) = \mu a(0) - \nu e^{i\theta} a^\dagger(0), \tag{55}$$

$$b(z) = \mu b(0) + \nu e^{-i\theta} b^\dagger(0), \tag{56}$$

where $\theta = \arg(\bar{\mu}^* \bar{\nu})$. (The preceding condition includes, but is not restricted to, the special case in which the pumps are linearly polarized, and the input signal is linearly polarized at 45° to the pumps.) Equations (55) and (56) describe two separate one-mode squeezing transformations of the form (14). The squeezing axes are different, but are not perpendicular. If the input signal is the coherent state $|\beta\rangle$, the output signal is a squeezed coherent state characterized by Eqs. (23)–(25), with ν replaced by $-\nu e^{i\theta}$ and $\alpha = \mu\beta - \nu e^{i\theta}\beta^*$.

4. Cascaded four-wave mixing processes

The degenerate FWM, or PC, processes described in Sections 2 and 3 produce squeezing because the frequency-matching condition $\omega_2 = (\omega_3 + \omega_1)/2$ ensures that the signal operator is coupled to its conjugate. However, if $\omega_2 \neq (\omega_3 + \omega_1)/2$, the signal operator is coupled to the conjugate operator of an idler mode with frequency $\omega_3 + \omega_1 - \omega_2 \neq \omega_2$. Squeezing requires the prior use of BS, or FC, to generate an idler that is a frequency-shifted, but non-conjugated, image of the signal. Once the idler has been generated by FC, PC can be used to produce squeezing. The scalar and vector versions of these cascaded nondegenerate-FWM processes are illustrated in Figure 6.

Consider the first-stage FC process. Like the nondegenerate FWM process described in Section 3, FC is subject to the frequency-matching condition $\omega_2 + \omega_3 = \omega_4 + \omega_1$. Unlike the aforementioned process, waves 1 and 3 are the pumps (rather than 1 and 4), wave 2 is the signal and wave 4 is the idler (rather than wave 3). FC is governed by the Hamiltonian

$$H = i\delta(a_2^\dagger a_2 - a_4^\dagger a_4) + i(\gamma a_2^\dagger a_4 + \gamma^* a_2 a_4^\dagger), \tag{57}$$

where γ depends on the pump amplitudes, together with the Heisenberg equations (46). Formulas for δ and γ are stated in [6, 8, 9, 10]. By combining Eqs. (46) and (57), one

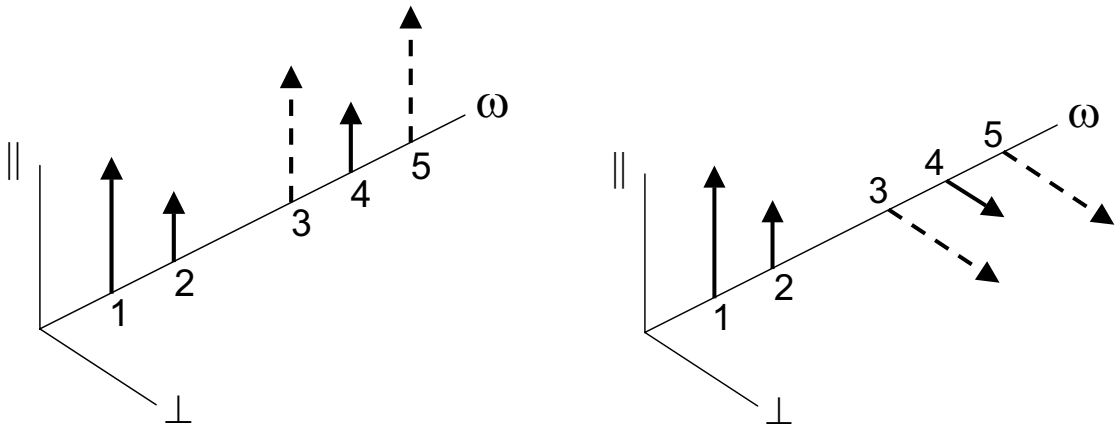

Figure 6: Polarization diagrams for cascaded scalar and vector FC and PC. During FC pump 3 is on and pump 5 is off, whereas during PC pump 3 is off and pump 5 is on.

obtains the operator equations

$$d_z a_2 = i\delta a_2 + i\gamma a_4, \tag{58}$$

$$d_z a_4 = i\gamma^* a_2 - i\delta a_4. \tag{59}$$

The solutions of Eqs. (58) and (59) are

$$a_2(z') = \bar{\mu}(z')a_2(0) + \bar{\nu}(z')a_4(0), \tag{60}$$

$$a_4(z') = -\bar{\nu}^*(z')a_2(0) + \bar{\mu}^*(z')a_4(0), \tag{61}$$

where the transfer functions

$$\bar{\mu}(z) = \cos(kz) + i(\delta/k)\sin(kz), \tag{62}$$

$$\bar{\nu}(z) = i(\gamma/k)\sin(kz) \tag{63}$$

and the wavenumber $k = (|\gamma|^2 + \delta^2)$. The transfer functions satisfy the auxiliary equation $|\bar{\mu}|^2 + |\bar{\nu}|^2 = 1$, which ensures that the FC transformation is unitary and conserves photons. Equations (60) and (61) are identical to the change-of-basis equations used in Section 3 and the beam-splitter equations. If the input signal is a coherent state with amplitude β_2, and the input idler is the vacuum state, the output is the two-mode coherent state$|\bar{\mu}\beta_2, -\bar{\nu}^*\beta_2\rangle$.

Now consider the second-stage PC process, which involves two pumps (5 and 1), and a signal (2) and idler (4), whose frequencies satisfy the matching condition $\omega_5 + \omega_1 = \omega_2 + \omega_4$.

[The first-pump and signal frequencies ω_1 and ω_2 were chosen at the input, and the idler frequency $\omega_4 = \omega_2+\omega_3-\omega_1$ was determined by the BS process, so the second-pump frequency $\omega_5 = \omega_3 + 2(\omega_2 - \omega_1)$.] PC is characterized by Eqs. (45)–(50), with the idler subscript 3 replaced by the subscript 4 (and the implicit pump subscript 4 replaced by the subscript 5), the initial distance 0 replaced by z' and the final distance z replaced by $z'' - z'$. Formulas for δ and γ are stated in [6, 7, 8, 9, 10]. If the input is a two-mode coherent state, the output is a two-mode squeezed coherent state. However, squeezing exists as correlations between the output modes: Neither output mode is squeezed by itself [12]. To demonstrate this important fact, let $\alpha_2 = \mu\bar{\mu}\beta_2 - \nu\bar{\nu}\beta_2^*$. Then, by following the procedure described before Eq. (16), one finds that the signal-operator moments are

$$\langle a_2 \rangle = \alpha_2, \tag{64}$$

$$\langle a_2^2 \rangle = \alpha_2^2, \tag{65}$$

$$\langle a_2^\dagger a_2 \rangle = |\alpha_2|^2 + |\nu|^2, \tag{66}$$

$$\langle (a_2^\dagger a_2)^2 \rangle = (|\alpha_2|^2 + |\nu|^2)^2 + |\alpha_2|^2(|\mu|^2 + |\nu|^2) + |\mu|^2|\nu|^2. \tag{67}$$

It follows from Eqs. (64)–(67) that

$$\langle \delta x_2^2 \rangle = (|\mu|^2 + |\nu|^2)/4, \tag{68}$$

$$\langle \delta y_2^2 \rangle = (|\mu|^2 + |\nu|^2)/4, \tag{69}$$

$$\langle \delta n_2^2 \rangle = |\alpha_2|^2(|\mu|^2 + |\nu|^2) + |\mu|^2|\nu|^2. \tag{70}$$

The quadrature and number variances depend on the magnitudes of α_2, μ and ν, but not the phases. ($|\alpha_2|^2$ depends on the phases of the input signal and the transfer coefficients.) The idler results are similar. If one applies FC and PC at the end of a link, one can use the correlated idler to manipulate (squeeze) the signal prior to detection. However, if one applies FC and PC at an intermediate point, dispersion in the remainder of the link causes the signal and idler pulses to walk off. (Even in a dispersion-managed system, in which the path-averaged dispersion is of order 1 ps/Km-nm, the arrival times of two pulses with a wavelength separation of 10 nm differ by 10^4 ps after propagation through 1000 Km of fiber.) Retrieving the idler is not practical. (Even if it were, the different sequences of pulse

collisions experienced by the signal and idler would weaken the correlations between them and, hence, would limit the extent to which the signal could be manipulated.)

One can also use FC to combine the signal and idler produced by prior PC. As described above, PC is subject to the frequency-matching condition $\omega_5 + \omega_1 = \omega_2 + \omega_4$, and FC is subject to the condition $\omega_2 + \omega_3 = \omega_4 + \omega_1$. In both processes wave 2 is the signal and wave 4 is the idler. By combining Eqs. (49) and (50), with z replaced by z', and Eqs. (60) and (61), with 0 replaced by z' and z' replaced by $z'' - z'$, one finds that

$$a_2(z'') = \mu\bar{\mu}a_2(0) + \nu\bar{\nu}a_2^\dagger(0) + \mu\bar{\nu}a_4(0) + \nu\bar{\mu}a_4^\dagger(0), \tag{71}$$

$$a_4(z'') = -\mu\bar{\nu}^*a_2(0) + \nu\bar{\mu}^*a_2^\dagger(0) + \mu\bar{\mu}^*a_4(0) - \nu\bar{\nu}^*a_4^\dagger(0), \tag{72}$$

where overbars denote the FC transfer-functions. By themselves, Eqs. (71) and (72) are difficult to interpret. However, one can rewrite the coherent input state $|\beta_2, 0\rangle$ as $R^\dagger(\gamma,\delta)$ $R(\gamma,\delta)|\beta_2, 0\rangle = R^\dagger(\gamma,\delta)|\bar{\mu}\beta_2, -\bar{\nu}^*\beta_2\rangle$, where $R(\gamma,\delta)$ is the redistribution (change-of-basis, beam-splitter or FC) operator. The properties of the redistribution operator are described briefly in Appendix A. Replacing the actual input $|\beta_2, 0\rangle$ by the virtual input $|\bar{\mu}\beta_2, -\bar{\nu}^*\beta_2\rangle$ is equivalent to making the operator replacements

$$a_2(0) \rightarrow \bar{\mu}^*a_2(0) - \bar{\nu}a_4(0), \tag{73}$$

$$a_4(0) \rightarrow \bar{\nu}^*a_2(0) + \bar{\mu}a_4(0) \tag{74}$$

in Eqs. (71) and (72). By making these replacements, one obtains the modified input-output relations

$$a_2(z) = \mu(|\bar{\mu}|^2 + |\bar{\nu}|^2)a_2(0) + \nu(2\bar{\mu}\bar{\nu})a_2^\dagger(0) + \nu(|\bar{\mu}|^2 - |\bar{\nu}|^2)a_4^\dagger(0), \tag{75}$$

$$a_4(z) = \nu(|\bar{\mu}|^2 - |\bar{\nu}|^2)a_2^\dagger(0) + \mu(|\bar{\mu}|^2 + |\bar{\nu}|^2)a_4(0) - \nu(2\bar{\mu}^*\bar{\nu}^*)a_4^\dagger(0). \tag{76}$$

One can also obtain Eqs. (75) and (76) from Eqs. (53) and (54), respectively, by making the replacements $\bar{\mu} \rightarrow \bar{\mu}^*$ and $\bar{\nu} \rightarrow -\bar{\nu}$. These replacements reflect the fact that the forward and backward change-of-basis and FC transformations are made in the opposite order. If the FC process redistributes photons equally ($|\bar{\mu}| = |\bar{\nu}| = 1/2$), Eqs. (75) and (76) reduce to

$$a_2(z) = \mu a_2(0) + \nu e^{i\theta}a_2^\dagger(0), \tag{77}$$

$$a_4(z) = \mu a_4(0) - \nu e^{-i\theta}a_4^\dagger(0), \tag{78}$$

where $\theta = \arg(\bar{\mu}\bar{\nu})$. Equations (77) and (78) describe two separate one-mode squeezing transformations of the form (14). If the input signal is the coherent state $|\beta_2\rangle$, the output signal and idler are squeezed coherent states characterized by Eqs. (23)–(25). For the signal ν is replaced by $\nu e^{i\theta}$ and $\alpha_2 = \mu(\bar{\mu}\beta_2) + \nu e^{i\theta}(\bar{\mu}\beta_2)^*$, whereas for the idler ν is replaced by $-\nu e^{-i\theta}$ and $\alpha_4 = -\mu(\bar{\nu}^*\beta_2) + \nu e^{-i\theta}(\bar{\nu}^*\beta_2)^*$. By using the fact that $|\bar{\mu}| = |\bar{\nu}|$, one can rewrite the signal and idler amplitudes as $\mu\bar{\mu}\beta_2 + \nu\bar{\nu}\beta_2^*$ and $-\mu\bar{\nu}^*\beta_2 + \nu\bar{\mu}^*\beta_2^*$, respectively. Notice that the signal and idler are squeezed by the same amount: One can squeeze the signal, or squeeze and frequency-convert it simultaneously.

5. Effects of polarization misalignment

In Section 3 it was shown that, if the polarization of the input signal is aligned perfectly, degenerate vector FWM produces an output signal that is a one-mode squeezed state. However, if the input signal is misaligned, the output signal cannot be characterized so simply. It is important to determine how the characteristics (lower-order operator moments) of the output signal depend on the polarization of the input signal. Let $a_1^\dagger = a^\dagger$, $a_2 = a$ and $a_3^\dagger = b^\dagger$. Then Eq. (53) can be written in the form

$$a_2(z) = \mu_{21}a_1^\dagger(0) + \mu_{22}a_2(0) + \mu_{23}a_3^\dagger(0), \tag{79}$$

where the composite transfer coefficients

$$\mu_{21} = -\nu(2\bar{\mu}^*\bar{\nu}), \quad \mu_{22} = \mu, \quad \mu_{23} = \nu(|\bar{\mu}|^2 - |\bar{\nu}|^2). \tag{80}$$

In Eqs. (80) μ and ν are the transfer coefficients associated with FWM, for which the natural modes are polarized parallel and perpendicular to the pumps, and $\bar{\mu}$ and $\bar{\nu}$ are the transfer coefficients associated with the change from the input basis (modes a and b) to the natural basis. It is easy to verify that $-|\mu_{21}|^2 + |\mu_{22}|^2 - |\mu_{23}|^2 = 1$, which ensures that the composite transformation is unitary. Equation (79) describes a phase-sensitive three-mode process (in which modes 1 and 2 are the same). We describe it colloquially as a process in which a phase-sensitive signal is coupled to a phase-insensitive idler. The characteristics of phase-insensitive three-mode processes (in which modes 1–3 are different) were described in [14].

By using the vacuum state as a virtual input state, and incorporating the coherent displacement required to produce the actual input state in the input-output relation associated with degenerate vector FWM, one obtains the modified input-output relation

$$a_2(z) = \alpha + \mu_{21} a_1^\dagger(0) + \mu_{22} a_2(0) + \mu_{23} a_3^\dagger(0), \tag{81}$$

where the output amplitude $\alpha = \mu_{21}\beta^* + \mu_{22}\beta$ and β is the input amplitude. It is now a simple matter to calculate the signal-operator moments. The results are

$$\begin{aligned}
\langle a_2 \rangle &= \alpha, && (82)\\
\langle a_2^2 \rangle &= \alpha^2 + \mu_{21}\mu_{22}, && (83)\\
\langle a_2^\dagger a_2 \rangle &= |\alpha|^2 + |\mu_{21}|^2 + |\mu_{23}|^2, && (84)\\
\langle (a_2^\dagger a_2)^2 \rangle &= (|\alpha|^2 + |\mu_{21}|^2 + |\mu_{23}|^2)^2 + |\alpha\mu_{22}^* + \alpha^*\mu_{21}|^2 \\
&\quad + |\alpha|^2|\mu_{23}|^2 + 2|\mu_{21}|^2|\mu_{22}|^2 + |\mu_{22}|^2|\mu_{23}|^2. && (85)
\end{aligned}$$

It follows from Eqs. (83) and (84), and the definitions $x = (a + a^\dagger)/2$ and $y = (a - a^\dagger)/2i$, that the quadrature variances

$$\begin{aligned}
\langle \delta x_2^2 \rangle &= (1 + 2|\mu_{21}|^2 + 2|\mu_{23}|^2 + \mu_{21}\mu_{22} + \mu_{21}^*\mu_{22}^*)/4, && (86)\\
\langle \delta y_2^2 \rangle &= (1 + 2|\mu_{21}|^2 + 2|\mu_{23}|^2 - \mu_{21}\mu_{22} - \mu_{21}^*\mu_{22}^*)/4. && (87)
\end{aligned}$$

It follows from Eqs. (84) and (85) that the number variance

$$\begin{aligned}
\langle \delta n_2^2 \rangle &= |\alpha\mu_{22}^* + \alpha^*\mu_{21}|^2 + |\alpha|^2|\mu_{23}|^2 + 2|\mu_{21}|^2|\mu_{22}|^2 + |\mu_{22}|^2|\mu_{23}|^2 \\
&= |\alpha|^2(|\mu_{21}|^2 + |\mu_{22}|^2 + |\mu_{23}|^2) + \alpha^2\mu_{21}^*\mu_{22}^* + (\alpha^*)^2\mu_{21}\mu_{22} \\
&\quad + 2|\mu_{21}|^2|\mu_{22}|^2 + |\mu_{22}|^2|\mu_{23}|^2. && (88)
\end{aligned}$$

Formulas for the idler-operator (mode 3) moments are derived in the Appendix.

Despite their complexity, the preceding results simplify considerably when rewritten in terms of the constituent transfer coefficients. The operator moments are

$$\begin{aligned}
\langle a_2^2 \rangle &= \alpha^2 - 2\mu\nu\bar{\mu}^*\bar{\nu}, && (89)\\
\langle a_2^\dagger a_2 \rangle &= |\alpha|^2 + |\nu|^2, && (90)
\end{aligned}$$

where the amplitude $\alpha = \mu\beta - 2\nu\bar{\mu}^*\bar{\nu}\beta^*$, and the quadrature and number variances are

$$\langle \delta q_2^2 \rangle = [1 + 2|\nu|^2 \mp (2\mu\nu\bar{\mu}^*\bar{\nu}) \mp (2\mu\nu\bar{\mu}^*\bar{\nu})^*]/4, \tag{91}$$

$$\begin{aligned} \langle \delta n_2^2 \rangle &= |\alpha|^2(|\mu|^2 + |\nu|^2) - \alpha^2(2\mu\nu\bar{\mu}^*\bar{\nu})^* \\ &\quad - (\alpha^*)^2(2\mu\nu\bar{\mu}^*\bar{\nu}) + |\mu|^2|\nu|^2(1 + 4|\bar{\mu}|^2|\bar{\nu}|^2). \end{aligned} \tag{92}$$

In Eq. (91) the $-$ signs apply to the x variance, whereas the $+$ signs apply to the y variance. When $|\bar{\mu}| = 1$ and $\bar{\nu} = 0$, Eqs. (89)–(92) reduce to the phase-insensitive equations (8), (9), (11) and (12). In contrast, when $|\bar{\mu}|^2 = 1/2$ and $|\bar{\nu}|^2 = 1/2$, Eqs. (89)–(92) reduce to the standard phase-sensitive equations (18)–(22) of [10]. By using the notation described in Section 2, one can rewrite the output strength- and phase-equations in the form

$$|\alpha|^2 = |\beta|^2\{G + 4(G-1)T(1-T) - 4[G(G-1)T(1-T)]^{1/2}\cos\xi\}, \tag{93}$$

$$\phi_\alpha = \phi_\beta + \phi_\mu - \tan^{-1}\Big\{\frac{2[(G-1)T(1-T)]^{1/2}\sin\xi}{G^{1/2} - 2[(G-1)T(1-T)]^{1/2}\cos\xi}\Big\}, \tag{94}$$

where $T = |\bar{\mu}|^2$ is the change-of-basis parameter and the relative phase $\xi = \phi_\nu + \phi_{\bar{\nu}} - 2\phi_\beta$. If $T = 1$ (0) the input signal is polarized parallel to pump 1 (4), and if $T = 1/2$ the parallel and perpendicular components of the input signal have equal magnitudes. As implied by Eq. (90), the output number is related to the output strength by Eq. (3). One can rewrite the quadrature- and number-variance equations in the form

$$\langle \delta q_2^2 \rangle = \{2G - 1 \mp 4[G(G-1)T(1-T)]^{1/2}\cos\eta\}/4, \tag{95}$$

$$\begin{aligned} \langle \delta n_2^2 \rangle &= |\alpha|^2\{2G - 1 - 4[G(G-1)T(1-T)]^{1/2}\cos\zeta\} \\ &\quad + G(G-1)[1 + 4T(1-T)], \end{aligned} \tag{96}$$

where the phases $\eta = \phi_\nu + \phi_{\bar{\nu}} + 2\phi_\mu$ and $\zeta = \phi_\nu + \phi_{\bar{\nu}} - 2(\phi_\alpha - \phi_\mu)$. It follows from Eq. (94) and the preceding definition that

$$\zeta = \xi + 2\tan^{-1}\Big\{\frac{2[(G-1)T(1-T)]^{1/2}\sin\xi}{G^{1/2} - 2[(G-1)T(1-T)]^{1/2}\cos\xi}\Big\}. \tag{97}$$

The following figures all pertain to the case in which μ is real ($\phi_\mu = 0$), the input number $|\beta|^2 = 100$ and the gain $G = 10$. In Figure 4 the output strength $|\alpha|^2$ and phase shift $\phi_\alpha - \phi_\beta$ are plotted as functions of the relative phase $\phi_\nu + \phi_{\bar{\nu}} - 2\phi_\beta$, for several values of

the transmittance T. The output strength is normalized to the output strength for PIA, which is given by Eq. (13). Because formulas (93) and (94) are symmetric functions of $T - 1/2$, it is not necessary to display results for $T > 1/2$. In Figure 5 the x variance is

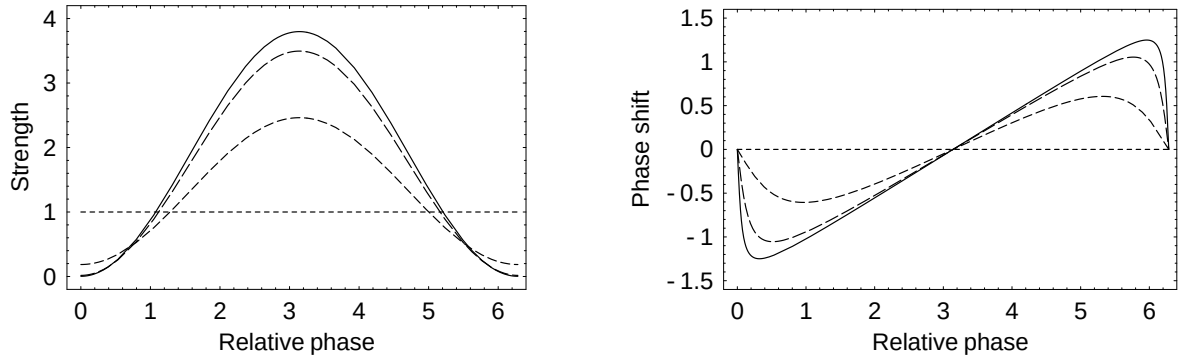

Figure 7: Signal strength and phase shift plotted as functions of the relative phase. The solid, long- and short-dashed, and dotted curves represent $T = 0.5$, 0.3, 0.1 and 0.0, respectively.

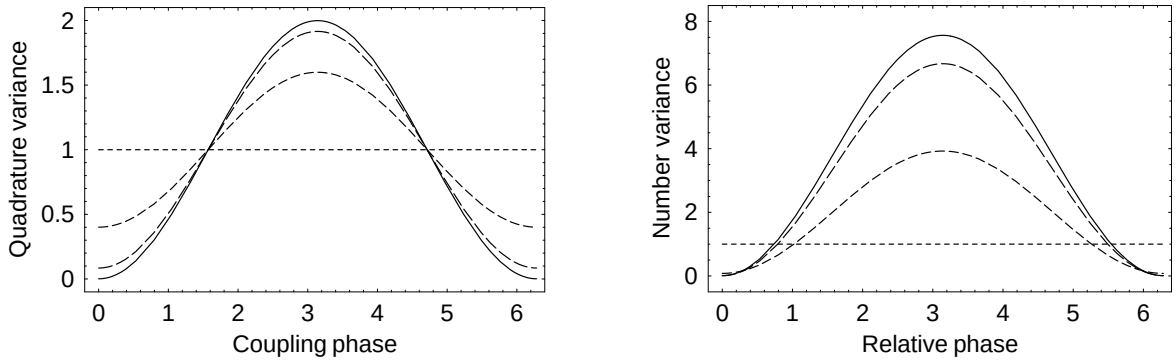

Figure 8: Signal quadrature and number variances plotted as functions of the coupling phase and relative phase, respectively. The solid, long- and short-dashed, and dotted curves represent $T = 0.5$, 0.3, 0.1 and 0.0, respectively.

plotted as a function of the coupling phase $\phi_\nu + \phi_{\bar{\nu}}$ and the number variance is plotted as a function of $\phi_\nu + \phi_{\bar{\nu}} - 2\phi_\beta$. Both variances are normalized to the variances for PIA, which are given by Eqs. (16) and (17). In Figure 6 the figure of demerit (defined in Section 2) is plotted as a function of $\phi_\nu + \phi_{\bar{\nu}} - 2\phi_\beta$. The results for $T = 0.5$ are similar to those for the standard one-mode squeezed state, which were illustrated in Figures 1–3. In fact, the only difference between these sets of results is their dependence on the relative phase (which is

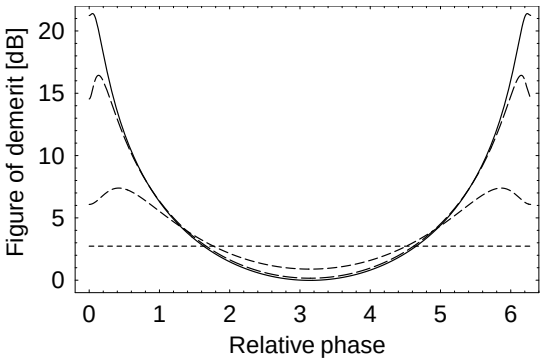

Figure 9: Figures of demerit for degenerate vector FWM. The solid, long- and short-dashed, and dotted curves represent $T = 0.5$, 0.3, 0.1 and 0.0, respectively.

shifted by π radians). The differences between the cases in which $T = 0.5$ and 0.3 (or 0.7) are finite, but small: The phase-sensitivity of degenerate vector FWM depends only weakly on deviations from the optimal value of T. For example, changing T from 0.5 to 0.3 increases the figure of demerit for out-of-phase amplification by only 0.2 dB. As T tends to 0 (or 1), the characteristics of degenerate vector FWM tend to those of PIA.

6. Effects of unbalanced conversion

In Section 4 it was shown that FC followed by PC produces one two-mode squeezed state. Changing the efficiency of the conversion process changes the amplitudes of the signal and idler that are the inputs for the PC process. However, these input modes remain coherent states, so the output modes remain parts of a two-mode squeezed state: FC followed by PC produces one two-mode squeezed state, for arbitrary conversion efficiencies.

It was also shown that, if the conversion process is balanced (the output strengths of the signal and idler are equal), PC followed by FC produces two one-mode squeezed states. However, if the conversion process is unbalanced, the output signal and idler cannot be characterized so simply. It is important to determine how the characteristics (lower-order operator moments) of the output signal and idler depend on the efficiency of the conversion process. Let $a_1^\dagger = a_2^\dagger$ and $a_3^\dagger = a_4^\dagger$. Then Eq. (71) can be written in the form

$$a_2(z) = \mu_{21} a_1^\dagger(0) + \mu_{22} a_2(0) + \mu_{23} a_3^\dagger(0) + \mu_{24} a_4(0), \tag{98}$$

where the composite transfer coefficients

$$\mu_{21} = \nu\bar{\nu}, \quad \mu_{22} = \mu\bar{\mu}, \quad \mu_{23} = \nu\bar{\mu}, \quad \mu_{24} = \mu\bar{\nu}. \tag{99}$$

In Eqs. (99) μ and ν are the transfer coefficients associated with PC, and $\bar{\mu}$ and $\bar{\nu}$ are the transfer coefficients associated with FC. It is easy to verify that $-|\mu_{21}|^2 + |\mu_{22}|^2 - |\mu_{23}|^2 + |\mu_{24}|^2 = 1$, which ensures that the composite transformation is unitary. Equation (98) describes a phase-sensitive four-mode process (in which modes 1 and 2 are the same, and modes 3 and 4 are the same). We describe it colloquially as a process in which a phase-sensitive signal is coupled to a phase-sensitive idler. The characteristics of phase-insensitive four-mode processes (in which modes 1–4 are different) were described in [14].

By using the vacuum state as a virtual input state, and incorporating the coherent displacement required to produce the actual input state in the input-output relation associated with PC followed by FC, one obtains the modified input-output relation

$$a_2(z) = \alpha_2 + \mu_{21}a_1^\dagger(0) + \mu_{22}a_2(0) + \mu_{23}a_3^\dagger(0) + \mu_{24}a_4(0), \tag{100}$$

where the output amplitude $\alpha_2 = \mu_{21}\beta_2^* + \mu_{22}\beta_2$ and β_2 is the input amplitude. It is now a simple matter to calculate the signal-operator moments. The results are

$$\langle a_2 \rangle = \alpha_2, \tag{101}$$

$$\langle a_2^2 \rangle = \alpha_2^2 + \mu_{21}\mu_{22} + \mu_{23}\mu_{24}, \tag{102}$$

$$\langle a_2^\dagger a_2 \rangle = |\alpha_2|^2 + |\mu_{21}|^2 + |\mu_{23}|^2, \tag{103}$$

$$\begin{aligned}\langle (a_2^\dagger a_2)^2 \rangle &= (|\alpha_2|^2 + |\mu_{21}|^2 + |\mu_{23}|^2)^2 + |\alpha_2\mu_{22}^* + \alpha_2^*\mu_{21}|^2 + |\alpha_2\mu_{24}^* + \alpha_2^*\mu_{23}|^2 \\ &\quad + |\mu_{22}^*\mu_{23} + \mu_{24}^*\mu_{21}|^2 + 2|\mu_{21}|^2|\mu_{22}|^2 + 2|\mu_{23}|^2|\mu_{24}|^2.\end{aligned} \tag{104}$$

It follows from Eqs. (102) and (103), and the definitions $x = (a + a^\dagger)/2$ and $y = (a - a^\dagger)/2i$, that the quadrature variances

$$\langle \delta x_2^2 \rangle = [1 + 2|\mu_{21}|^2 + 2|\mu_{23}|^2 + (\mu_{21}\mu_{22} + \mu_{23}\mu_{24}) + (\mu_{21}\mu_{22} + \mu_{23}\mu_{24})^*]/4, \tag{105}$$

$$\langle \delta y_2^2 \rangle = [1 + 2|\mu_{21}|^2 + 2|\mu_{23}|^2 - (\mu_{21}\mu_{22} + \mu_{23}\mu_{24}) - (\mu_{21}\mu_{22} + \mu_{23}\mu_{24})^*]/4. \tag{106}$$

It follows from Eqs. (103) and (104) that the number variance

$$\langle \delta n_2^2 \rangle = |\alpha_2\mu_{22}^* + \alpha_2^*\mu_{21}|^2 + |\alpha_2\mu_{24}^* + \alpha_2^*\mu_{23}|^2$$

$$
\begin{aligned}
&+ |\mu_{22}^{*}\mu_{23} + \mu_{24}^{*}\mu_{21}|^2 + 2|\mu_{21}|^2|\mu_{22}|^2 + 2|\mu_{23}|^2|\mu_{24}|^2 \\
= \;& |\alpha_2|^2(|\mu_{21}|^2 + |\mu_{22}|^2 + |\mu_{23}|^2 + |\mu_{24}|^2) + \alpha_2^2(\mu_{21}\mu_{22} + \mu_{23}\mu_{24})^* \\
&+ (\alpha_2^*)^2(\mu_{21}\mu_{22} + \mu_{23}\mu_{24}) + 2|\mu_{21}|^2|\mu_{22}|^2 + 2|\mu_{23}|^2|\mu_{24}|^2 \\
&+ |\mu_{22}\mu_{23}|^2 + |\mu_{24}\mu_{21}|^2 + (\mu_{21}\mu_{22})(\mu_{23}\mu_{24})^* + (\mu_{21}\mu_{22})^*(\mu_{23}\mu_{24}). \qquad (107)
\end{aligned}
$$

For the (mathematical) case in which $\mu_{24} = 0$, the four-mode equations (101)–(107) reduce to the three-mode equations (82)–(88). For the (mathematical) case in which $\mu_{21} = 0$, Eqs. (101)–(107) describe the characteristics of a phase-insensitive signal coupled to a phase-sensitive idler. Formulas for the idler-operator (mode 4) moments are derived in Appendix B.

Despite their complexity, the preceding results simplify considerably when rewritten in terms of the constituent transfer functions. The operator moments are

$$
\begin{aligned}
\langle a_2^2 \rangle &= \alpha_2^2 + 2\mu\nu\bar{\mu}\bar{\nu}, \qquad (108) \\
\langle a_2^{\dagger} a_2 \rangle &= |\alpha_2|^2 + |\nu|^2, \qquad (109)
\end{aligned}
$$

where the amplitude $\alpha_2 = \mu\bar{\mu}\beta_2 + \nu\bar{\nu}\beta_2^*$, and the quadrature and number variances are

$$
\begin{aligned}
\langle \delta q_2^2 \rangle &= [1 + 2|\nu|^2 \pm (2\mu\nu\bar{\mu}\bar{\nu}) \pm (2\mu\nu\bar{\mu}\bar{\nu})^*]/4, \qquad (110) \\
\langle \delta n_2^2 \rangle &= |\alpha_2|^2(|\mu|^2 + |\nu|^2) + \alpha_2^2(2\mu\nu\bar{\mu}\bar{\nu})^* \\
&\quad + (\alpha_2^*)^2(2\mu\nu\bar{\mu}\bar{\nu}) + |\mu|^2|\nu|^2(1 + 4|\bar{\mu}|^2|\bar{\nu}|^2). \qquad (111)
\end{aligned}
$$

In Eq. (110) the + signs apply to the x variance, whereas the − signs apply to the y variance. When $|\bar{\mu}| = 1$ and $\bar{\nu} = 0$, Eqs. (108)–(111) reduce to the phase-insensitive equations (8), (9), (11) and (12). In contrast, when $|\bar{\mu}|^2 = 1/2$ and $|\bar{\nu}|^2 = 1/2$, Eqs. (108)–(111) reduce to the standard phase-sensitive equations (18)–(22) of [10]. By using the notation described in Section 2, one can rewrite the output strength- and phase-equations in the form

$$
\begin{aligned}
|\alpha_2|^2 &= |\beta_2|^2\{GT + (G-1)(1-T) + 2[G(G-1)T(1-T)]^{1/2}\cos\xi\}, \qquad (112) \\
\phi_\alpha &= \phi_\beta + \phi_\mu + \phi_{\bar{\mu}} + \tan^{-1}\left\{\frac{[(G-1)(1-T)]^{1/2}\sin\xi}{(GT)^{1/2} + [(G-1)(1-T)]^{1/2}\cos\xi}\right\}, \qquad (113)
\end{aligned}
$$

where $T = |\bar{\mu}|^2$ is the frequency-conversion parameter and the relative phase $\xi = \phi_\nu + \phi_{\bar{\nu}} - 2\phi_\beta$. If $T = 1$ (0) no (complete) conversion occurs, and if $T = 1/2$ the output strengths of the signal and idler are equal. As implied by Eq. (109), the output number is related

to the output strength by Eq. (3). One can rewrite the quadrature- and number-variance equations in the form

$$\langle \delta q_2^2 \rangle = \{2G - 1 \pm 4[G(G-1)T(1-T)]^{1/2} \cos\eta\}/4, \tag{114}$$

$$\langle \delta n_2^2 \rangle = |\alpha_2|^2 \{2G - 1 + 4[G(G-1)T(1-T)]^{1/2} \cos\zeta\}, + G(G-1)[1 + 4T(1-T)], \tag{115}$$

where the phases $\eta = \phi_\nu + \phi_{\bar{\nu}} + 2(\phi_\mu + \phi_{\bar{\mu}})$ and $\zeta = \phi_\nu + \phi_{\bar{\nu}} - 2(\phi_\alpha - \phi_\mu - \phi_{\bar{\mu}})$. It follows from Eq. (113) and the preceding definition that

$$\zeta = \xi - 2\tan^{-1}\left\{\frac{[(G-1)(1-T)]^{1/2}\sin\xi}{(GT)^{1/2} + [(G-1)(1-T)]^{1/2}\cos\xi}\right\}. \tag{116}$$

The following figures all pertain to the case in which μ and $\bar{\mu}$ are real ($\phi_\mu = 0$ and $\phi_{\bar{\mu}} = 0$), the input number $|\beta|^2 = 100$ and the gain $G = 10$. In Figure 7 the output strength $|\alpha_2|^2$ and phase shift $\phi_\alpha - \phi_\beta$ are plotted as functions of the relative phase $\phi_\nu + \phi_{\bar{\nu}} - 2\phi_\beta$, for several values of the transmittance T. The output strength is normalized to the output

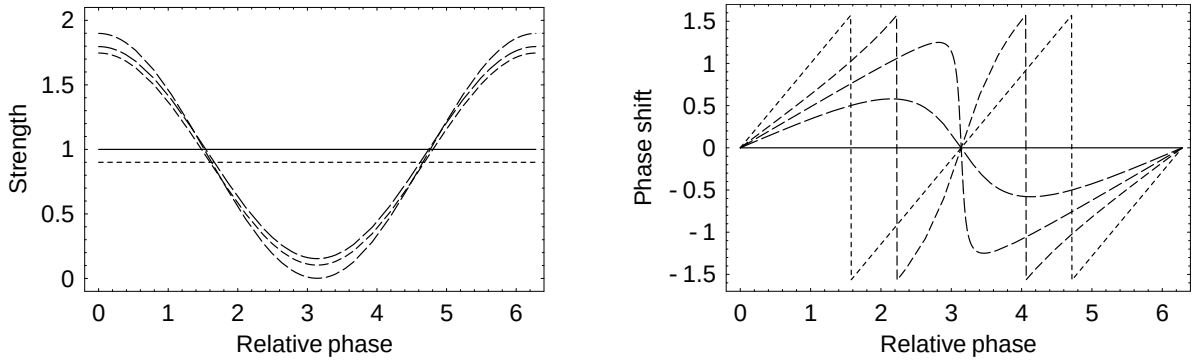

Figure 10: Signal strength and phase shift plotted as functions of the relative phase. The solid, long-, medium- and short-dashed, and dotted curves represent $T = 1.00$, 0.75, 0.50, 0.10 and 0.00, respectively.

strength for PIA, which is given by Eq. (13). In Figure 8 the x variance is plotted as a function of the coupling phase $\phi_\nu + \phi_{\bar{\nu}}$ and the number variance is plotted as a function of $\phi_\nu + \phi_{\bar{\nu}} - 2\phi_\beta$. Both variances are normalized to the variances for PIA, which are given by Eqs. (16) and (17). Because the x variance is a symmetric function of $T - 1/2$ the (omitted) curves for $T = 0.75$ and 1.00 are identical to the (included) curves for $T = 0.25$ and 0.00,

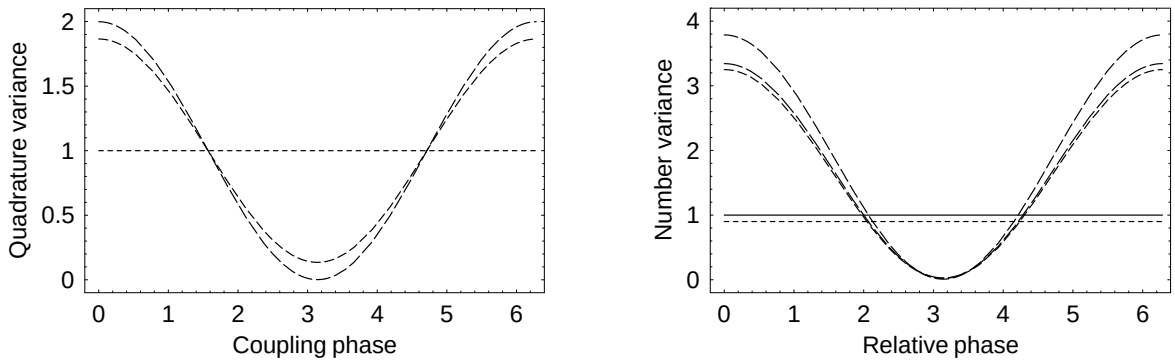

Figure 11: Signal quadrature and number variances plotted as functions of the coupling phase and relative phase, respectively. The solid, long-, medium- and short-dashed, and dotted curves represent $T = 1.00$, 0.75, 0.50, 0.10 and 0.00, respectively.

respectively. In Figure 9 the figure of demerit (defined in Section 2) is plotted as a function of $\phi_\nu + \phi_{\bar{\nu}} - 2\phi_\beta$. The results for $T = 0.5$ are similar to those for the standard one-mode squeezed

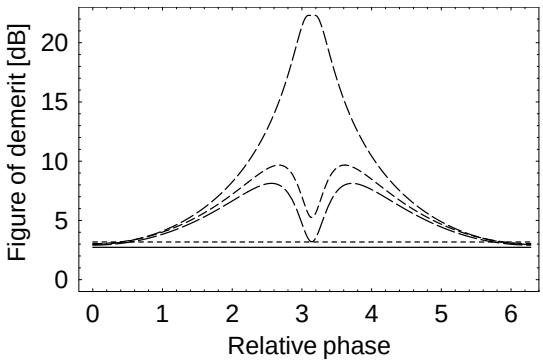

Figure 12: Figures of demerit for PC followed by FC. The solid, long-, medium- and short-dashed, and dotted curves represent $T = 1.00$, 0.75, 0.50, 0.10 and 0.00, respectively.

state, which were illustrated in Figures 1–3. The differences between these sets of results are caused by the differences between the output strengths (numbers). In the standard PSA process the number increase varies between 0 and $4G$ (in the high-gain regime), whereas in PC followed by FC it varies between 0 and $2G$. By itself, PC provides a total (signal and idler) number increase of $2G$. The FC process redistributes photons between the signal and idler, but does not change the total number. Consequently, the number increase produced by PC followed by FC must vary between 0 and $2G$. [Photon conservation also requires the output numbers of the signal and idler to vary inversely.] The differences between the cases

in which $T = 0.25$, 0.5 and 0.75 are finite, but small: The phase-sensitivity of PC followed by FC depends only weakly on deviations from the optimal value of T. For example, changing T from 0.50 to 0.75 changes the figure of demerit for in-phase amplification by only 0.06 dB. (To leading order in G, the figure of demerit for in-phase amplification is independent of T.) As T tends to 1 (or 0) the signal characteristics of PC followed by FC tend to the signal (idler) characteristics of PIA.

7. Summary

In this paper some quantum-mechanical aspects of phase-sensitive amplification (PSA) in a fiber were discussed. Four schemes that provide PSA were studied, each of which is based on four-wave mixing (FWM).

Degenerate scalar FWM converts a coherent input-state (signal) into a one-mode squeezed coherent output-state, which is suitable for retransmission. Degenerate vector FWM performs the same function if the polarization vector of the input signal is aligned perfectly. Phase conjugation (PC) followed by Bragg scattering (BS), or frequency conversion (FC), converts a coherent input-state into two one-mode squeezed coherent output-states (signal and frequency-shifted idler) if the conversion process is balanced. Both output states are suitable for retransmission. Thus, devices based on degenerate FWM or PC followed by FC can be used to provide PSA at intermediate points in a fiber link, or to manipulate (squeeze) a signal at the end of the link, prior to detection.

In contrast, FC followed by PC converts a coherent input-state into a two-mode squeezed coherent output-state. Squeezing exists as correlations between the output-states: Neither the signal nor the idler is squeezed by itself, so neither is suitable for retransmission. However, FC followed by PC can be used at the end of a link to squeeze a signal prior to detection.

For each scheme, formulas were derived for the field-quadrature and photon-number variances, which facilitate the (signal and idler) noise-figure analyses for direct and homodyne detection [13]. The effects of polarization misalignment on degenerate vector FWM and the effects of unbalanced conversion on PC followed by FC were also studied. As the amounts of these imperfections increase, the phase-sensitivities of the amplification processes decrease. However, for moderate imperfections the performance degradations are small: Degenerate

vector FWM and PC followed by FC can tolerate moderate amounts of polarization misalignment and unbalanced conversion.

Appendix A: Displacement, squeezing and redistribution operators

In this appendix the properties of displacement, squeezing and redistribution operators are reviewed briefly. The simplest nontrivial Hamiltonian that involves a mode operator can be written in the form

$$H = -iga^\dagger + ig^* a, \tag{117}$$

where g is a constant. By combining Eqs. (12) and (117), one obtains the (Heisenberg) operator equation

$$d_z a = ga, \tag{118}$$

which has the simple solution

$$a(z) = a(0) + \alpha, \tag{119}$$

where the displacement $\alpha = gz$. According to Eq. (10), this displacement is produced by the (Schrödinger) transformation operator $D = e^{iHz}$. It follows from this definition and Eq. (117) that the displacement operator

$$D(\alpha) = \exp(\alpha a^\dagger - \alpha^* a). \tag{120}$$

Because H is hermitian, the conjugate operator $(e^{iHz})^\dagger = e^{-iHz}$. Consequently, one can verify solution (119) by using Eq. (10) and the operator identity

$$e^{-o} a e^{o} = a + [a, o] + [[a, o], o]/2! + [[[a, o], o], o]/3! + \ \ldots \tag{121}$$

For the displacement operator, $o = \alpha a^\dagger - \alpha^* a$ and

$$[a, o] = \alpha. \tag{122}$$

Because α is a constant, the series in Eq. (121) truncates at the second term and

$$D^\dagger(\alpha) a D(\alpha) = a + \alpha, \tag{123}$$

which is equivalent to Eq. (119). For any forward-transformation operator e^{iHz}, the backward-transformation operator is e^{-iHz}: The backward operator is obtained from the forward operator by the replacement of z with $-z$. This propagation-reversal symmetry implies that

$D^\dagger(\alpha) = D(-\alpha)$. It follows from Eq. (123) and the preceding relation that

$$D(\alpha)aD^\dagger(\alpha) = a - \alpha. \tag{124}$$

In Section 2 it was shown that degenerate scalar FWM produces a one-mode squeezed state. It follows from Eqs. (7) and (9) that the squeezing operator

$$S(\delta, \gamma) = \exp[i\delta a^\dagger a + i(\gamma a^{\dagger 2} + \gamma^* a^2)/2], \tag{125}$$

where γ and δ are constants, which contain the distance factor z implicitly. For this one-mode squeezing operator

$$[a, o] = i\delta a + i\gamma a^\dagger, \tag{126}$$

$$[[a, o], o] = (|\gamma|^2 - \delta^2)a. \tag{127}$$

Because the second-order commutator is proportional to a, the higher-order commutators are related to the first- and second-order commutators in a simple way. By retaining the first three terms on the right side of Eq. (121), one finds that

$$S^\dagger(\delta, \gamma)aS(\delta, \gamma) \approx [(1 + \kappa^2/2!) + i\delta(1 + \kappa^2/3!)]a + i\gamma(1 + \kappa^2/3!)a^\dagger, \tag{128}$$

where $\kappa = (|\gamma|^2 - \delta^2)^{1/2}$. The contributions $(1 + \kappa^2/2!)$ and $(1 + \kappa^2/3!)$ are the first two terms in the Taylor expansions of $\cosh \kappa$ and $(\sinh \kappa)/\kappa$, respectively. It follows from these facts that

$$S^\dagger(\gamma, \delta)aS(\gamma, \delta) = \mu(\gamma, \delta)a + \nu(\gamma, \delta)a^\dagger, \tag{129}$$

where μ and ν are the transfer functions defined in Eqs. (5) and (6), respectively. It follows from propagation-reversal symmetry and the transfer-function formulas that

$$S(\gamma, \delta)aS(\gamma, \delta)^\dagger = \mu^*(\gamma, \delta)a - \nu(\gamma, \delta)a^\dagger. \tag{130}$$

The standard way to create a squeezed coherent state is to displace a squeezed vacuum state: $|\alpha, \gamma, \delta\rangle = D(\alpha)S(\gamma, \delta)|0\rangle$. It follows from Eqs. (123) and (129) that the mode operator associated with this process

$$S^\dagger(\gamma, \delta)D^\dagger(\alpha)aD(\alpha)S(\gamma, \delta) = \mu a + \nu a^\dagger + \alpha. \tag{131}$$

The alternative way to create such a state is to squeeze a coherent state: $|\beta,\gamma,\delta\rangle = S(\gamma,\delta)D(\beta)|0\rangle$. The associated mode operator

$$D^\dagger(\beta)S^\dagger(\gamma,\delta)aS(\gamma,\delta)D(\beta) = \mu a + \nu a^\dagger + \mu\beta + \nu\beta^*. \tag{132}$$

It follows from Eqs. (131) and (132) that the two processes are equivalent if

$$\alpha = \mu\beta + \nu\beta^*. \tag{133}$$

Condition (133) is equivalent to the condition

$$\beta = \mu^*\alpha - \nu\alpha^*. \tag{134}$$

In Section 3 it was shown that degenerate vector FWM produces a two-mode squeezed state. It follows from Eqs. (9) and (45) that the squeezing operator

$$S(\gamma,\delta) = \exp[i\delta(a_1^\dagger a_1 + a_2^\dagger a_2) + i(\gamma a_1^\dagger a_2^\dagger + \gamma^* a_1 a_2)], \tag{135}$$

where γ and δ are constants, which contain the distance factor implicitly, and the subscripts 2 and 3 were replaced by the standard subscripts 1 and 2, respectively. For this two-mode squeezing operator

$$[a_1, o] = i\delta a_1 + i\gamma a_2^\dagger, \tag{136}$$

$$[[a_1, o], o] = (|\gamma|^2 - \delta^2)a_1. \tag{137}$$

The commutators that involve a_2 are similar. By proceeding as described between Eqs. (127) and (130), one finds that

$$S^\dagger(\gamma,\delta)a_1 S(\gamma,\delta) = \mu(\gamma,\delta)a_1 + \nu(\gamma,\delta)a_2^\dagger, \tag{138}$$

$$S(\gamma,\delta)a_1 S^\dagger(\gamma,\delta) = \mu^*(\gamma,\delta)a_1 - \nu(\gamma,\delta)a_2^\dagger. \tag{139}$$

Because the squeezing operator (135) is a symmetric function of a_1 and a_2, the results for mode 2 follow from Eqs. (138) and (139) by the interchange of the subscripts 1 and 2. (In the forward transformation of $a_2^\dagger$, μ and ν are replaced by ν^* and μ^*, respectively, whereas in the backward transformation μ^* and $-\nu$ are replaced by $-\nu^*$ and μ, respectively.)

One can produce a two-mode squeezed coherent state by displacing twice a two-mode squeezed vacuum state, or by squeezing two coherent states. By proceeding as described between Eqs. (131) and (133), one finds that the states $|\alpha_1, \alpha_2, \gamma, \delta\rangle = D(\alpha_2)D(\alpha_1)S(\gamma, \delta)|0, 0\rangle$ and $|\beta_1, \beta_2, \gamma, \delta\rangle = S(\gamma, \delta)D(\beta_2)D(\beta_1)|0, 0\rangle$ are equivalent if

$$\alpha_1 = \mu\beta_1 + \nu\beta_2^*, \tag{140}$$

$$\alpha_2^* = \nu^*\beta_1 + \mu^*\beta_2^*. \tag{141}$$

Conditions (140) and (141) are equivalent to the conditions

$$\beta_1 = \mu^*\alpha_1 - \nu\alpha_2^*, \tag{142}$$

$$\beta_2^* = -\nu^*\alpha_1 + \mu\alpha_2^*. \tag{143}$$

In Section 4 it was shown that a change of basis and frequency conversion both produce the same (beam-splitter) transformation of a pair of input states. It follows from Eqs. (9) and (57) that the redistribution operator

$$R(\gamma, \delta) = \exp[i\delta(a_1^\dagger a_1 - a_2^\dagger a_2) + i(\gamma a_1^\dagger a_2 + \gamma^* a_1 a_2^\dagger)], \tag{144}$$

where δ and γ are constants, which contain the distance factor implicitly, and the subscripts 2 and 4 were changed to the standard subscripts 1 and 2, respectively. For this two-mode redistribution operator

$$[a_1, o] = i\delta a_1 + i\gamma a_2, \tag{145}$$

$$[[a_1, o], o] = -(|\gamma|^2 + \delta^2)a_1. \tag{146}$$

The commutators that involve a_2 are similar (δ and γ are replaced by $-\delta$ and γ^*, respectively). By proceeding as described between Eqs. (127) and (130), one finds that

$$R^\dagger(\gamma, \delta)a_1 R(\gamma, \delta) = \bar{\mu}(\gamma, \delta)a_1 + \bar{\nu}(\gamma, \delta)a_2, \tag{147}$$

$$R(\gamma, \delta)a_1 R^\dagger(\gamma, \delta) = \bar{\mu}^*(\gamma, \delta)a_1 - \bar{\nu}(\gamma, \delta)a_2, \tag{148}$$

where $\bar{\mu}$ and $\bar{\nu}$ are the transfer functions defined in Eqs. (62) and (63), respectively. The results for mode 2 are similar. (In the forward transformation $\bar{\mu}$ and $\bar{\nu}$ are replaced by $-\bar{\nu}^*$ and $\bar{\mu}^*$, respectively, whereas in the backward transformation $\bar{\mu}^*$ and $-\bar{\nu}$ are replaced by $\bar{\nu}^*$ and $\bar{\mu}$, respectively.)

In Section 4 use was made of the fact that the redistribution operator converts one pair of coherent states into another pair. The two-mode coherent state $|\alpha_1, \alpha_2\rangle = D(\alpha_2)D(\alpha_1)|0,0\rangle$. For this standard displacement process the associated mode operators are $a_1+\alpha_1$ and $a_2+\alpha_2$. By using the fact that $R(\gamma,\delta)|0,0\rangle = |0,0\rangle$, which follows from definition (144), one can rewrite the coherent state as $D(\alpha_2)D(\alpha_1)R(\gamma,\delta)|0,0\rangle$. It follows from Eqs. (123) and (147) that the first mode operator associated with this alternative displacement process

$$R^\dagger(\gamma,\delta)D^\dagger(\alpha_1)D^\dagger(\alpha_2)a_1 D(\alpha_2)D(\alpha_1)R(\gamma,\delta) = \bar{\mu}a_1 + \bar{\nu}a_2 + \alpha_1. \tag{149}$$

The formula for the second mode operator is similar. Now consider the state produced by the action of $R(\gamma,\delta)D(\beta_2)D(\beta_1)$ on $|0,0\rangle$. The first mode operator associated with this displacement and redistribution process

$$D^\dagger(\beta_1)D^\dagger(\beta_2)R^\dagger(\gamma,\delta)a_1 R(\gamma,\delta)D(\beta_2)D(\beta_1) = \bar{\mu}a_1 + \bar{\nu}a_2 + \bar{\mu}\beta_1 + \bar{\nu}\beta_2. \tag{150}$$

The formula for the second mode operator is similar. It follows from Eqs. (149) and (150), and their counterparts for mode 2, that the state in question is a two-mode coherent state with amplitudes

$$\alpha_1 = \bar{\mu}\beta_1 + \bar{\nu}\beta_2, \tag{151}$$

$$\alpha_2 = -\bar{\nu}^*\beta_1 + \bar{\mu}^*\beta_2. \tag{152}$$

Equations (151) and (152) are equivalent to the equations

$$\beta_1 = \bar{\mu}^*\alpha_1 - \bar{\nu}\alpha_2, \tag{153}$$

$$\beta_2 = \bar{\nu}^*\alpha_1 + \bar{\mu}\alpha_2. \tag{154}$$

In this appendix relations between certain pairs of transformations were established by comparisons of the (Heisenberg) mode operators associated with the concatenated transformations. One can also establish these relations by comparing the associated (Schrödinger) transformation operators. These comparisons are facilitated by the identity

$$U^\dagger f(a)U = f(U^\dagger a U), \tag{155}$$

which allows one to rewrite a modified transformation operator as a transformation operator with a modified argument. For example, $D(\alpha)S(\gamma,\delta) = S(\gamma,\delta)D(\beta)$ if and only if $D(\alpha) =$

$S(\gamma,\delta)D(\beta)S^{\dagger}(\gamma,\delta)$. By using identity (155) to make the similarity transformation, one finds that the equivalence condition is $\alpha=\mu\beta+\nu\beta^{*}$, in agreement with Eq. (133). Finally, when $\delta=0$, the results derived in this appendix reduce to the textbook results [12, 13].

Appendix B: Characteristics of the generated idlers

In Sections 5 and 6 the output characteristics of the amplified signals were studied. In this appendix the output characteristics of the generated idlers are analyzed. First, consider degenerate vector FWM. Equation (54) can be written in the form

$$a_4(z)=\mu_{41}a_1^{\dagger}(0)+\mu_{43}a_2(0)+\mu_{43}a_3^{\dagger}(0)+\mu_{44}a_4(0), \tag{156}$$

where the mode operators $a_1^{\dagger}=a^{\dagger}$, $a_2=a$, $a_3^{\dagger}=b^{\dagger}$ and $a_4=b$, and the composite transfer coefficients

$$\mu_{41}=\nu(|\bar{\mu}|^2-|\bar{\nu}|^2),\quad \mu_{42}=0,\quad \mu_{43}=\nu(2\bar{\mu}\bar{\nu}^{*}),\quad \mu_{44}=\mu. \tag{157}$$

Second, consider PC followed by FC. Equation (72) can also be written in the form of Eq. (156), where the mode operators $a_1^{\dagger}=a_2^{\dagger}$ and $a_3^{\dagger}=a_4^{\dagger}$, and the composite transfer functions

$$\mu_{41}=\nu\bar{\mu}^{*},\quad \mu_{42}=-\mu\bar{\nu}^{*},\quad \mu_{43}=-\nu\bar{\nu}^{*},\quad \mu_{44}=\mu\bar{\mu}^{*}. \tag{158}$$

In both cases $-|\mu_{41}|^2+|\mu_{42}|^2-|\mu_{43}|^2+|\mu_{44}|^2=1$.

By using the vacuum state as a virtual input state, and incorporating the coherent displacement required to produce the actual input state in the input-output relation (156), one obtains the modified input-output relation

$$a_4(z)=\alpha_4+\mu_{41}a_1^{\dagger}(0)+\mu_{43}a_2(0)+\mu_{43}a_3^{\dagger}(0)+\mu_{44}a_4(0), \tag{159}$$

where $\alpha_4=\mu_{41}\beta_2^{*}+\mu_{42}\beta_2$. For degenerate vector FWM, $\alpha_4=\nu(|\bar{\mu}|^2-|\bar{\nu}|^2)$. The idler strength $|\alpha_4|^2$ and the total strength $|\alpha_2|^2+|\alpha_4|^2$ are both phase sensitive. For PC followed by FC, $\alpha_4=\nu\bar{\mu}^{*}\beta_2-\mu\bar{\nu}^{*}\beta_2^{*}$. Although the idler strength is phase sensitive, the total strength is phase insensitive (because FC redistributes photons produced by phase-insensitive PC). Equation (159) has the same form as Eq. (100), with α_2 replaced by α_4 and μ_{2j} replaced by μ_{4j}. Consequently, one can obtain formulas for the idler-operator moments by making the aforementioned substitutions in Eqs. (101)–(107).

References

[1] R. Loudon, "Theory of noise accumulation in linear optical-amplifier chains," IEEE J. Quantum Electron. **21**, 766–773 (1985).

[2] H. P. Yuen, "Reduction of quantum fluctuation and suppression of the Gordon–Haus effect with phase-sensitive linear amplifiers," Opt. Lett. **17**, 73–75 (1992).

[3] Y. Mu and C. M. Savage, "Parametric amplifiers in phase-noise-limited optical communications," J. Opt. Soc. Am. B **9**, 65–70 (1992).

[4] R. D. Li, P. Kumar, W. L. Kath and J. N. Kutz, "Combating dispersion with parametric amplifers," IEEE Photon. Technol. Lett. **5**, 669–672 (1993).

[5] W. Imajuku and A. Takada, "Reduction of fiber-nonlinearity-enhanced amplifier noise by means of phase-sensitive amplifiers," Opt. Lett. **22**, 31–33 (1997).

[6] C. J. McKinstrie, S. Radic and A. R. Chraplyvy, "Parametric amplifiers driven by two pump waves," IEEE J. Sel. Top. Quantum Electron. **8**, 538–547 and 956 (2002).

[7] C. J. McKinstrie, S. Radic and C. Xie, "Phase conjugation driven by orthogonal pump waves in birefringent fibers," J. Opt. Soc. Am. B **20**, 1437–1446 (2003).

[8] C. J. McKinstrie, S. Radic and C. Xie, "Parametric instabilities driven by orthogonal pump waves in birefringent fibers," Opt. Express **11**, 2619–2633 (2003).

[9] C. J. McKinstrie, H. Kogelnik, R. M. Jopson, S. Radic and A. V. Kanaev, "Four-wave mixing in fibers with random birefringence," Opt. Express **12**, 2033–2055 (2004).

[10] C. J. McKinstrie and S. Radic, "Phase-sensitive amplification in a fiber," Opt. Express **12**, 4973–4979 (2004).

[11] W. H. Louisell, *Radiation and Noise in Quantum Electronics* (McGraw-Hill, 1964).

[12] R. Loudon and P. L. Knight, "Squeezed light," J. Mod. Opt. **34**, 709–759 (1987).

[13] R. Loudon, *The Quantum Theory of Light, 3rd Ed.* (Oxford University Press, 2000).

[14] C. J. McKinstrie, S. Radic and M. G. Raymer, "Quantum noise properties of parametric amplifiers driven by two pump waves," Opt. Express **12**, 5037–5066 (2004).